Dissociation pathways established in strong-field single ionization of molecular CO

Guoqiang Shi[1] · Yulin Xiang[1] · Jianting Lei[1] · Shaohua Sun[1] · Zuoye Liu[1] · Bitao Hu[1]

Abstract

In this study, we present the dissociative single ionization of CO molecules in strong laser field by measuring the time-of-flight mass spectra of the dissociative fragment C^+ with different laser intensities and polarization directions, respectively. The results indicate that the molecular ion CO^+ produced by over-the-barrier ionization can be populated in not only the ground $X^2\Sigma^+$ state, but also the next two lower-lying electronic $A^2\Pi$ and $B^2\Sigma^+$ states. By evaluation of the potential energy curves, we assign the multi-peak structure of the time-of-flight spectra for ion fragment C^+ to the dissociation of the vibrational states of two excited $A^2\Pi$ and $B^2\Sigma^+$ states via the dissociation pathways $|A^2\Pi - 0\omega\rangle \rightarrow |D^2\Pi - 4\omega\rangle$, $|B^2\Sigma^+ - 0\omega\rangle \rightarrow |3^2\Pi - 3\omega\rangle$, and $|B^2\Sigma^+ - 0\omega\rangle \rightarrow |3^2\Sigma^+ - 3\omega\rangle$. The results imply that the dissociation pathway of molecular cations can be selected using pump-probe technology via accurately tuned laser parameters.

1 Introduction

With the advances of ultrashort pulsed lasers, many intriguing and essential physical phenomena have been observed in laser-matter interaction research, such as bond softening and hardening [1–3], above-threshold dissociation [4, 5], Coulomb explosion [6, 7], enhanced ionization [8, 9], and high harmonic generation [10, 11], etc. Theoretical models, e.g., Strong Field Approximation (SFA) [12], Molecular Ammosov-Delone-Krainov (MO-ADK) [13], and Time-Dependent Hartree-Fock (TDHF) [14] were introduced to study these phenomena. Compared with atoms, however, the cognition process of the experimental results for multielectron molecules is difficult and challenging due to the electronic, vibrational, rotational, and dissociative motions in the interaction between molecules and photons [15–18]. Several electrons can be removed from a molecule by intense laser fields. The coupling between the nuclear and the electron coordinates should be considered in the multiple ionization processes. Generally, the kinetic energy release (KER) and angular distribution of fragment ions are measured to investigate the highly charged dissociative ionization of molecules. A two-step Coulomb explosion model can qualitatively evaluate the total KER of fragment ions [19, 20]. The anisotropic angular distribution of fragment ions, which is observed to be strong signals along the laser polarization axis, can be attributed to two effects: geometric alignment and dynamic alignment. The geometric alignment is described as the ionization rate on the angle between the molecular axis and the laser polarization axis [20, 21] and the dynamic alignment is defined as a laser-induced reorientation of the molecules before or during the dissociative ionization [22–26]. Molecular dynamics is complicated in strong laser fields. Therefore, it is not easy to evaluate the importance of different orbitals, dissociation pathways, and the coupling between different excited states.

In recent years, molecular cations as the research object have attracted extensive attention, which are produced by single ionization; thus, there is no electron correlation effect. The single ionization of NO was studied by utilizing a time-of-flight mass spectroscopy (TOF-MS) technology [27]. It was found that the NO molecules, when oriented perpendicular to the laser polarization, appear to preferentially dissociate into the $N^+ + O$ channel rather than the $N + O^+$ channel, despite the energy level of the former channel being about 1 eV higher than the latter channel. Previously different research groups have experimentally investigated the dissociative ionization of CO molecules [26, 28–31]. The study of the single ionization of CO was mainly focused on

✉ Zuoye Liu
zyl@lzu.edu.cn

Bitao Hu
hubt@lzu.edu.cn

1   School of Nuclear Science and Technology, Lanzhou University, 730000, China

the multiphoton ionization region [28–30] and seldom concentrated on the tunnel ionization regime [31]. The physical model established in the study of multielectron dissociative ionization of molecules is not suitable for dissociative single ionization. Indeed, the unique electronic structure of the molecule and the lower-lying electronic states are coupled to the dissociative states by absorbing multiple photons, which play essential roles during the dissociative single ionization of molecules in strong field.

Here, we investigate the single ionization of CO in the over-the-barrier region and the subsequent dissociation channel $CO^+ \rightarrow C^+ + O$. The dissociation pathways of CO molecule cation are established by analyzing the total KER spectra observed for the dissociative fragment C^+ and the dependence of the TOF spectra of C^+ fragment ion on laser polarization angles and intensities. We conclude that two bonding orbitals $(1\pi)^4$ and $(4\sigma)^2$ are involved in the single ionization process and the strong coupling between different excited states has identified three dissociation pathways. It is confirmed that bonding orbitals and coupling effects play essential roles in the dissociative single ionization of CO molecules.

2 Experimental setup

The laser used in the experiment is a Ti:sapphire system that delivers 33 fs pulses at a 1 kHz repetition rate with the central wavelength at 800 nm. The incident laser beam is focused by an $f = 10$ cm spherical mirror in the vacuum chamber mounted on a 5-Axes Manipulator. The focal spot is adjusted to be in the center of the extraction region by the Manipulator. A half-wave plate and a Gran-Taylor prism are inserted into the path of the laser beam to vary the pulse energy. After taking away the prism, the polarization direction of the linearly polarized light can be changed from parallel (P-polarization) to perpendicular (S-polarization) to the TOF axis by rotating the half-wave plate. In the measurement, the polarization angle is defined as the angle between the laser polarization vector and the TOF axis. The CO gas (99.99%) is introduced into the vacuum chamber via a 30 μm orifice with a base pressure of 4.0×10^{-8} Pa, and the working pressure is about 1.0×10^{-7} Pa. The details of our experimental setup have been described elsewhere [32, 33]. Briefly, a schematic diagram of the experimental setup is shown in Fig. 1a. The TOF-MS is utilized to detect and collect the ions. The experimental system employed a dual-slope extraction field.

The ions are extracted, accelerated, and arrive at the MCP detector through a field-free region. The extraction and acceleration fields are 145 and 1020 V/cm, respectively. The diameter of the hole on plates 2 and 3 is 1.0 mm and 2.0 mm, respectively. Part of the charged particles can pass
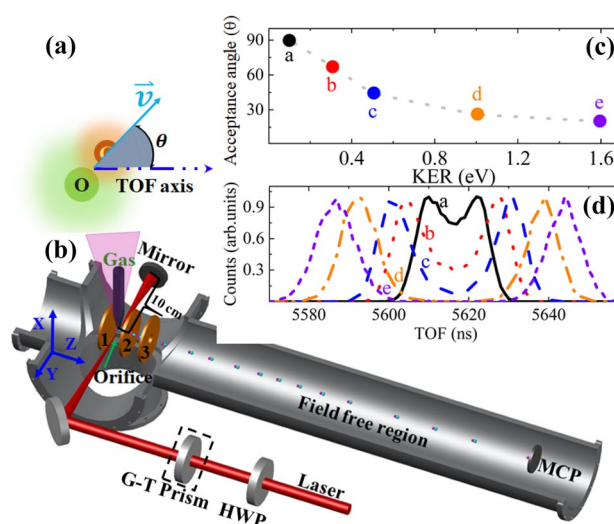
Fig. 1 **a** The acceptance angle θ is defined as the angle between the initial velocity ($\vec{v}$) of the fragment ion and the TOF axis. **b** Schematic diagram of the experimental setup. The applied voltages of plates 1 and 2 are 1200 and 1000 V, respectively, and the third plate is grounded. The acceptance angle (**c**) and TOF spectra (**d**) of C^+ ions at different kinetic energies are given by the Monte Carlo simulation

through the pinhole and arrive at the MCP detector due to the geometric effect of the pinhole. Here, the acceptance angle θ is defined as the angle between the TOF axis and the initial velocity of the fragment ion. The acceptance angle and TOF spectra of C^+ ions at different kinetic energies are obtained by Monte Carlo simulation, as shown in Fig. 1c and d, respectively. The MCP signal is converted to a digital signal by ADQ-412, and the digital signal is stored and processed offline to generate TOF mass spectra.

3 Results and discussion

Figure 2 shows the TOF mass spectra of CO induced by femtosecond laser pulses at a peak power density of 1.29×10^{15} W/cm^2, which is calibrated by the Ar^{2+}/Ar^+ yield ratio [34–37]. The laser electric field is P-polarization in Fig. 2a and S-polarization in Fig. 2b. The signals of C^{p+} (p=1-3), O^{q+} (q=1-2), and CO^+ can be realized. The previous article has systematically studied the dissociation process of highly charged molecular ions (CO^{q+}, q≥2) [33]. The molecular ion CO^+ will dissociate through the channel $CO^+ \rightarrow C^+ + O$ and $CO^+ \rightarrow C + O^+$. Since H_2O is difficult to be removed from the vacuum chamber, the middle peak of O^{q+} is from the multielectron dissociative ionization of H_2O. In CO, the O atom has a higher electronegativity than the C atom. On the other hand, the dissociation limit of the $C^+ + O$ (22.4 eV) channel is lower than that of the $C + O^+$ (24.7 eV) channel [38]. These two intuitive pictures predict that the $C^+ + O$

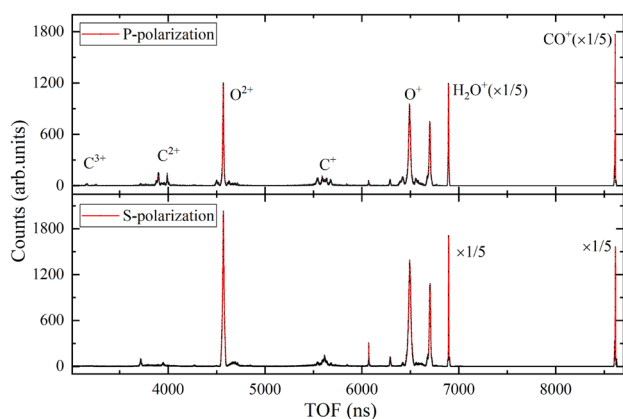**Fig. 2** TOF mass spectra of CO molecule irradiated at a laser intensity of 1.29×10^{15} W/cm^2. The peaks of H$_2$O$^+$ and CO$^+$ are multiplied by a factor of $\frac{1}{5}$. The laser polarization direction is parallel in **a** and perpendicular in **b** to the TOF axis

channel is more favorable than the C + O$^+$ channel. In conclusion, the O$^+$ ion peak corresponding to the weak channel C + O$^+$ overlaps with the O$^+$ ion peak produced by the residual water molecules in the vacuum chamber, resulting in the inability to extract the relevant information of the dissociation channel C + O$^+$. Thus, we focus on the dissociation channel C$^+$ + O in strong laser field.

Figure. 3a displays the typical TOF mass spectra of P-polarization and S-polarization of the C$^+$ region at a laser intensity of 1.29×10^{15} W/cm^2. Two dissociation channels principally contribute to the multi-peak structure, i.e., CO$^{2+} \rightarrow$ C$^+$ + O$^+$ (region I) and CO$^+ \rightarrow$ C$^+$ + O (region II). Note that, throughout this study, we label channel C$^+$ + O as C(1,0) or O(0,1),

and channel C$^+$ + O$^+$ as C(1,1) or O(1,1). We deduced the momentum of the neutral O atom using momentum conservation law, the kinetic energy of fragment ions can be determined from the peak splitting in the mass spectrum, and the total kinetic energy release (KER) is distributed between the two fragments, i.e., C$^+$ and O. The final total KER is

$$E_{KER} = \frac{m_o + m_c}{m_o} \times \frac{p^2(U_1 - U_2)^2}{8m_c d^2} \Delta t^2, \quad (1)$$

where U_1 is the potential of the plate 1, U_2 is the potential of the plate 2, d is the distance between these plates, p is the charge of the C$^+$, Δt is the difference in the arrival times between forward and backward ejected the C$^+$ ions, and m_o and m_c are the mass of the C and O atoms, respectively. Corresponding to Fig. 3a, the distribution of total KER of the dissociation channel C(1,0) is shown in Fig. 3b.

The momentum conservation law is satisfied in the process of the Coulomb explosion. Thus, the coincidence criterion of the dissociation channel of C(p,q) or O(q,p) can be given

$$p\Delta t_{C^{p+}} = q\Delta t_{O^{q+}}. \quad (2)$$

Here, $\Delta t_{C^{p+}}$ and $\Delta t_{O^{q+}}$ represent the difference in the arrival times between forward and backward ejected the C^{p+} and O^{q+} ions, respectively. The coincident spectra of C(1,1) or O(1,1) channels are displayed in Fig. 4. The C$^+$ ions come from the dissociation channel of C(1,1) in the region I by comparing the results in Fig. 3a and Fig. 4a. The dissociation of a highly charged molecular ion may also contribute to the C$^+$ ions at the intensity of 1.29×10^{15} W/cm^2. The dissociation channel of CO^{3+} ions is mainly C(2,1) or O(1,2) channel. Fig. 4b shows the coincident spectra of O$^+$ ions from O(1,1) and O(1,2) channels. For higher charged
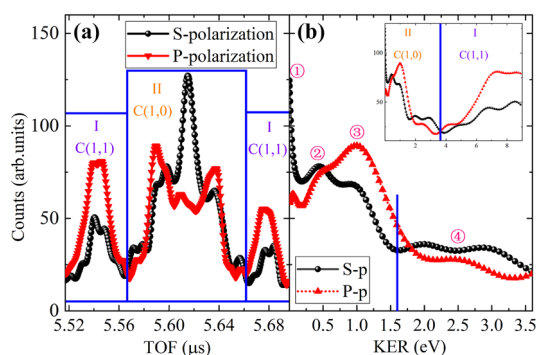

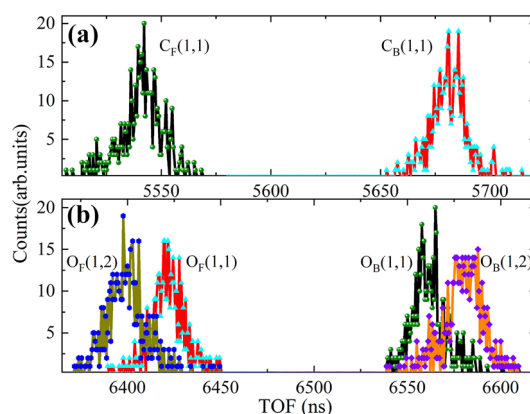**Fig. 3** **a** The TOF mass spectra of the dissociative fragment C$^+$ were measured at an intensity of 1.29×10^{15} W/cm^2. The lines with balls (black) and triangles (red) illustrate that the laser polarization direction is parallel to and perpendicular to the TOF axis, respectively. Region I and II refer to the C(1,1) and C(1,0) channels. **b** shows the corresponding total KER spectra by Eq. (1). The symbols ①–④ represent four energy peaks in channel C(1,0). The inset figure shows the total KER distribution of all fragment ions C$^+$, including the C(1,1) channel

Fig. 4 The **a** and **b** are the coincidence spectra of C$^+$ and O$^+$ ions corresponding to C(1,1) and C(2,1) channels, respectively. The subscripts F and B are defined as fragment ions with initial velocity toward and away from the detector. The same color of mass spectra of fragment ions is produced by the dissociation of the same parent molecule. Here, the spectrum of C^{2+} ion is not given

molecular ions (CO^{4+} and CO^{5+}), a previous study found that charge-symmetric dissociation is the dominant process [20]. Therefore, the contribution of other dissociation channels to C^+ can be ignored in present study. Based on the above discussion, we will focus on the dissociation pathway of the CO^+ in strong laser field.

From the total KER distribution of the C(1,0) channel in Fig. 3b, it can be seen that the KER distribution of region II can be divided into two parts, namely KER > 1.6 eV and KER < 1.6 eV, which will be explained later. To understand the physical mechanism of the CO cation dissociation process, we establish the strong field multiphoton dissociation pathways of CO^+. Fig. 5a shows the density distribution of TOF mass spectra of the C^+ with varying laser intensities. In Fig. 5, the observed asymmetry in the peak intensities is attributed to the vector addition of velocity of the fragment ions initially directed toward and away from the TOF axis [39]. Under the same laser intensity, the yield of the C^+ fragment in the high-energy part (③) is higher than that of the C^+ in the low-energy part (①, ②). This indicates
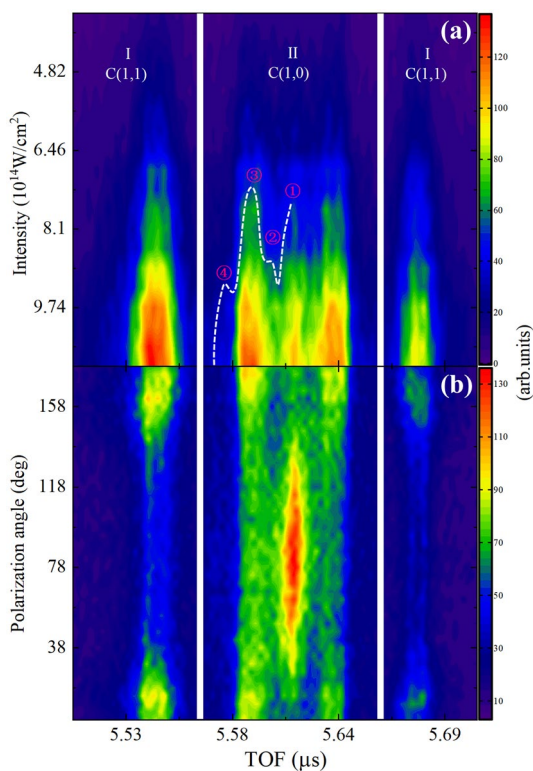

Fig. 5 **a** The TOF spectra of C^+ obtained at different laser intensities. The symbol ①-④ and ①-④ in Fig. 3b are one-to-one correspondence. The angle between the laser polarization direction and the TOF axis is fixed at 18°. **b** The TOF spectra of C^+ ion are measured at different polarization angles with a fixed laser intensity of 1.29×10^{15} W/cm². Here, the polarization angle refers to the angle between the laser polarization direction and the TOF axis

that the dissociation pathway corresponding to fragment ion C^+ of the lower energy part needs to absorb more photons. Moreover, the result in Fig. 5b reveals the density distribution of TOF mass spectra of the C^+ to polarization angle. In the ultrafast dissociation of diatomic molecule, the fragment anisotropy is determined by the direction of the transition moment respecting to the molecular axis [40, 41]. The rich electronic structure of CO^+ produces numerous distinct features, which gives us insight into the pathways. Compared with homonuclear diatomic molecules, heteronuclear diatomic molecules only need to obey the following molecular dipole transition selection rules. First, only the electronic states with the same multiplicity are allowed transition, i.e., $\Delta S = 0$. CO molecules have two sets of electronic states, doublet state and quartet state [42, 43]. Since the quartet state has higher ionization energy than the doublet state, we choose the doublet state. Second, $\Sigma^+ \leftrightarrow \Sigma^-$ transition is forbidden transition, i.e., $\sigma \leftrightarrow \sigma$ is forbidden. Third, the change of angular momentum quantum number $\Delta\Lambda = 0$ and $\Delta\Lambda = \pm1$ are defined as a parallel (e.g., $\Sigma \leftrightarrow \Sigma$, $\Pi \leftrightarrow \Pi$) and perpendicular (e.g., $\Sigma \leftrightarrow \Pi$) transitions. As shown in Fig. 5a, the structure of TOF mass spectra of C^+ has not changed obviously within the experimental energy range, indicating the production mechanism of C^+ ions remains unchanged. The acceptance angle of C^+ with higher kinetic energy is smaller, as shown in Fig. 1c. Therefore, it can be considered that the C^+ ions collected in the present experiment come from the dissociative single ionization of molecule with molecular axis along the TOF axis. In other words, changing the direction of the laser polarization relative to the TOF axis is equivalent to changing the angle between the direction of laser polarization and the molecular axis. Thus, it can be inferred that the dissociation pathway of CO^+ includes parallel and perpendicular transitions from the density distribution of C^+ TOF mass spectra with respect to laser polarization in Fig.5b.

The potential energy curves (PECs) of CO ground state and CO^+ ion are shown in Fig. 6c. The two dissociation limits of CO^+ ion are 22.37 eV and 24.34 eV, respectively [38]. The electronic configuration of CO is $(1\sigma)^2(2\sigma)^2(3\sigma)^2(4\sigma)^2(1\pi)^4(5\sigma)^2$. As CO is a heteronuclear diatomic molecule, unlike its isoelectronic counterpart N_2, the outermost orbital $(5\sigma)^2$ (highest occupied molecular orbital, HOMO) is virtually a nonbonding orbital. However, the two orbitals of $(1\pi)^4$ (HOMO-1) and $(4\sigma)^2$ (HOMO-2) are strongly bonding orbitals. Fig. 6b is the contour plots of the wave function of these orbitals. The CO molecules can only move thermally in the target chamber. The interval of the adjacent electronic states (several eV) and the interval of the adjacent vibrational state (~0.266 eV) are higher than k_BT (k_BT=0.026 eV at T=300 K). Hence, CO molecules are mainly populated in the ground state, $X^1\Sigma^+$ ($v' = 0$). From the point of view of electronic configuration, if we
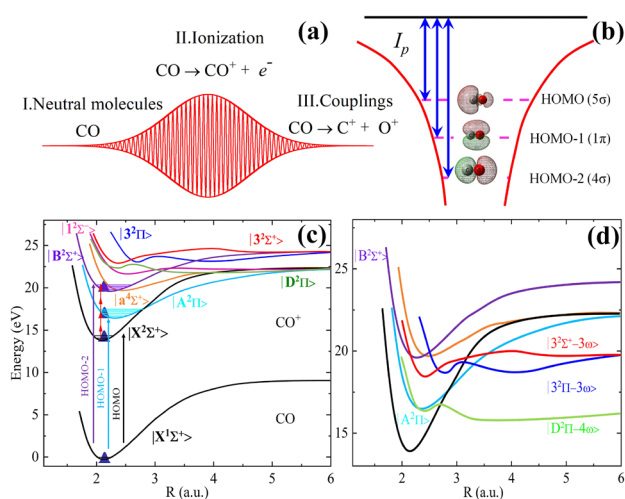
Fig. 6 **a** To make the physical image intuitive, the laser pulse can be divided into three regions qualitatively. **b** The configuration of the HOMO, HOMO-1, and HOMO-2 orbitals of CO and the contour maps of these orbital wave functions are from Ref. [48]. **c** The potential-energy surfaces of CO and CO^+ (taken from [42]). **d** Dressed-states of CO^+, lines with different colors refer to different transition pathways

remove an electron from the 5σ orbital, the remaining tightly bonding electrons should most likely hold the $X^2\Sigma^+$ ground state of the CO^+, which is a stable state. With the nondissociative molecular ion CO^+ formation, an abundance of CO molecular cations is observed in the experiments. The $A^2\Pi$ and $B^2\Sigma^+$ excited states are generated by removing a 1π and 4σ orbitals electron, respectively. Using the experimental results in Fig. 5 and the transition rules discussed above, a physical picture of the dissociative single ionization of CO is established, as shown in Fig. 6. To more intuitively and clearly understand the dissociative single ionization of CO molecule in the intense laser field, we divide the ionization and dissociation processes in a single laser pulse as shown in Fig. 6a. The physical processes in different stages cannot be strictly distinguished. First of all, most CO molecules remain neutral in the rising edge of the laser field as ionization is extremely sensitive to the laser intensity. In addition, when the intensity of the laser field reaches its peak, CO molecules are rapidly ionized and mainly populated in $X^2\Sigma^+$, $A^2\Pi$, and $B^2\Sigma^+$ electronic states. The ionization potentials of HOMO, HOMO-1, and HOMO-2 orbitals of CO molecule are 14.01, 16.58, and 19.70 eV, respectively [44]. The Keldysh parameters corresponding to HOMO, HOMO-1, and HOMO-2 are calculated to be 0.302, 0.328, and 0.358 with a laser intensity of 1.29×10^{15} W/cm^2, respectively [45]. However, CO molecules can be ionized by over-the-barrier at this laser peak intensity [46]. After ionization, CO^+ are populated to $X^2\Sigma^+$, $A^2\Pi$, and $B^2\Sigma^+$ electronic states. The Franck–Condon factor gives the vibrational state distribution

of different electronic states. The Franck-Condon factors of the transition between different electronic vibrational states of CO molecule are calculated by R. W. Nicholls [47]. The distributions of vibrational energy levels of $X^2\Sigma^+$, $A^2\Pi$, and $B^2\Sigma^+$ electronic states after CO ionized are $v'' = 0\text{-}1$, $v'' = 0\text{-}6$, and $v'' = 0\text{-}2$, respectively. As displayed in Fig. 6c, there is a four-photon near-resonant excitation between $X^2\Sigma^+$ and $B^2\Sigma^+$ states, increasing the population of CO molecular cations in the $B^2\Sigma^+$ state. Finally, the CO^+ ions populated in $A^2\Pi$ and $B^2\Sigma^+$ states are coupled with higher molecular states by absorbing multiple photons, and then CO^+ ions are dissociated.

Here, the diabatic Floquet representation is introduced, which gives diabatic filed-dressed PECs [40, 49–51]. The absorption of n photons will result in the shifting of the PECs down. This representation is adopted to illustrate the coupling of different dressed states. There are three dissociation pathways that can be distinguished in our experimental results, i.e., $|A^2\Pi - 0\omega\rangle \rightarrow |D^2\Pi - 4\omega\rangle$, $|B^2\Sigma^+ - 0\omega\rangle \rightarrow |3^2\Pi - 3\omega\rangle$, and $|B^2\Sigma^+ - 0\omega\rangle \rightarrow |3^2\Sigma^+ - 3\omega\rangle$. The dissociation limit of $|D^2\Pi - 4\omega\rangle$ state is about 0.51 eV which is lower than that of the $|A^2\Pi - 0\omega\rangle$ ($v'' = 0$, 16.68 eV) [44]. The Franck-Condon factor shows a maximum at $v'' = 2$ in the $|A^2\Pi - 0\omega\rangle$ vibrational state after CO single ionization. The corresponding total KER of $|A^2\Pi\rangle$ ($v'' = 2$, 17.06 eV) state is 0.89 eV, which is in good agreement with the ③ peak in Fig. 3b. As the interval between the two vibrational levels of $v'' = 0$, 6 in $A^2\Pi$ state is 1.09 eV, the maximum KER given by this dissociation pathway is 1.60 eV. For the dissociation pathway $|A^2\Pi - 0\omega\rangle \rightarrow |D^2\Pi - 4\omega\rangle$ is a parallel transition, because the change of angular momentum quantum number $\Delta\Lambda$ before and after the transition is 0. It can be seen from Fig. 5b that the yield of the C^+ ion corresponding to the ③ peak is the largest when the laser polarization direction is parallel to the TOF axis. This dissociation pathway gives a maximum KER of 1.6 eV, which is the reason for the division of region II into two parts in Fig. 3b mentioned earlier.

However, for $|3^2\Pi - 3\omega\rangle$ and $|3^2\Sigma^+ - 3\omega\rangle$ dressed states have the same dissociation limit of 19.69 eV. The energy of the vibrational level $|B^2\Sigma^+ - 0\omega\rangle$ ($v'' = 0$, 1, and 2) are 19.81, 20.01, and 20.22 eV [44]. The three KER values contributed by two dissociation pathways are 0.12, 0.32, and 0.53 eV, respectively. According to the transition rule, the $|B^2\Sigma^+ - 0\omega\rangle \rightarrow |3^2\Pi - 3\omega\rangle$ is perpendicular transition and the $|B^2\Sigma^+ - 0\omega\rangle \rightarrow |3^2\Sigma^+ - 3\omega\rangle$ is parallel transition. It can be seen faintly from Fig. 5b that the ② peak has the highest yield of the C^+ when the laser polarization is perpendicular to the TOF axis. This result shows that the main contribution of the ② peak comes from the $|B^2\Sigma^+ - 0\omega\rangle \rightarrow |3^2\Pi - 3\omega\rangle$ dissociation pathway. Although the $|B^2\Sigma^+ - 0\omega\rangle \rightarrow |3^2\Sigma^+ - 3\omega\rangle$ dissociation

pathway can also contribute to the ② peak, it is a parallel transition. The $|3^2\Sigma^+ - 3\omega\rangle$ potential energy curve has a small barrier, which weakens the contribution of the $|B^2\Sigma^+ - 0\omega\rangle \rightarrow |3^2\Sigma^+ - 3\omega\rangle$ dissociation pathway to the ② peak. Therefore, the fragment ions corresponding to the ② peak principally come from the dissociation of the $|B^2\Sigma^+ - 0\omega\rangle \rightarrow |3^2\Pi - 3\omega\rangle$ pathway.

Finally, we discuss the source of the ① peak in Fig. 5b, the initial kinetic energy of the fragment ion C^+ is close to 0 eV, and the yield for C^+ is the largest when the laser polarization direction is perpendicular to the TOF axis. As shown in Fig. 1c, the kinetic energy of the dissociated fragment C^+ is close to zero, and its acceptance angle is close to 90°. For the CO molecules whose molecular axis is perpendicular to the TOF axis, the component of the initial kinetic energy of the C^+ in the direction of the TOF is equal to 0 eV. Thus, the contribution of the ① peak mainly comes from the $|B^2\Sigma^+ - 0\omega\rangle \rightarrow |3^2\Sigma^+ - 3\omega\rangle$ dissociation pathway. It can be seen from Fig. 5a that the ④ peak appears at higher laser intensity than the ② peak. The dependence of the two peaks ② and ④ on the laser polarization is the same, the C^+ has the highest yield when the laser polarization direction is perpendicular to the TOF axis in Fig. 5b. According to the previous discussion, it is concluded that the source of the ④ peak absorbs one more photon than the ② peak, i.e., the $|B^2\Sigma^+ - 0\omega\rangle \rightarrow |3^2\Pi - 4\omega\rangle$ dissociation pathway. The observation indicates molecular inner orbitals are also involved in the single ionization process of CO. The different excited states of the CO molecular cations are coupled to form different dissociation pathways that depend on laser properties, such as polarization and intensity.

4 Conclusion

In summary, the multiorbital single ionization and the subsequent dissociation of CO molecule in an intense laser field have been studied. The established three dissociation pathways confirm that the two lower-lying electronic states $A^2\Pi$ and $B^2\Sigma^+$, play an important role during the dissociation of CO molecular cation. The dependence of fragment ions on laser polarization is determined by the transition manner (parallel or perpendicular) of the dissociation pathways. The molecular inner orbitals (HOMO-1 and HOMO-2) have a non-negligible influence on strong-field molecular single ionization. High-resolution measurements of vibrational levels in an electronic state are challenging during the dissociation of molecular cation in a strong field, because the involvement of an abundance of electronic states and possibly different dissociation pathways could bring about the fragment ions of same energy. The analysis of these results

shows that the dissociative pathway of molecular cation can be selected by using the pump-probe technique.

Disclosures

Conflict of interest The authors declare no conflicts of interest.

References

1. P.H. Bucksbaum, A. Zavriyev, H.G. Muller, D.W. Schumacher, Softening of the H_2^+ molecular bond in intense laser fields. Phys. Rev. Lett. **64**, 1883–1886 (1990)
2. A. Zavriyev, P.H. Bucksbaum, J. Squier, F. Saline, Light-induced vibrational structure in H_2^+ and D_2^+ in intense laser fields. Phys. Rev. Lett. **70**, 1077–1080 (1993)
3. L.J. Frasinski, J.H. Posthumus, J. Plumridge, K. Codling, P.F. Taday, A.J. Langley, Manipulation of bond hardening in H_2^+ by chirping of intense femtosecond laser pulses. Phys. Rev. Lett. **83**, 3625–3628 (1999)
4. Annick Giusti-Suzor, Xin He, Osman Atabek, Frederic H. Mies, Above-threshold dissociation of h 2+ in intense laser fields. Phys. Rev. Lett. **64**(5), 515 (1990)
5. Lu. Peifen, Junping Wang, Hui Li, Kang Lin, Xiaochun Gong, Qiying Song, Qinying Ji, Wenbin Zhang, Junyang Ma, Hanxiao Li et al., High-order above-threshold dissociation of molecules. Proc. Natl. Acad. Sci. **115**(9), 2049–2053 (2018)
6. B.D. Esry, A.M. Sayler, P.Q. Wang, K.D. Carnes, I. Ben-Itzhak, Above threshold coulomb explosion of molecules in intense laser pulses. Phys. Rev. Lett. **97**, 013003 (2006)
7. B. Manschwetus, T. Nubbemeyer, K. Gorling, G. Steinmeyer, U. Eichmann, H. Rottke, W. Sandner, Strong laser field fragmentation of H_2: Coulomb explosion without double ionization. Phys. Rev. Lett. **102**, 113002 (2009)
8. T. Zuo, A.D. Bandrauk, Charge-resonance-enhanced ionization of diatomic molecular ions by intense lasers. Phys. Rev. A **52**, R2511–R2514 (1995)
9. E. Constant, H. Stapelfeldt, P.B. Corkum, Observation of enhanced ionization of molecular ions in intense laser fields. Phys. Rev. Lett. **76**, 4140–4143 (1996)
10. Anne L'Huillier, M. Lewenstein, P. Salières, Ph. Balcou, MYu. Ivanov, J. Larsson, C.G. Wahlström, High-order harmonic-generation cutoff. Phys. Rev. A **48**, R3433–R3436 (1993)
11. Tsuneto Kanai, Eiji J. Takahashi, Yasuo Nabekawa, Katsumi Midorikawa, Destructive interference during high harmonic generation in mixed gases. Phys. Rev. Lett. **98**, 153904 (2007)
12. J. Muthbohm, A. Becker, Farhard Faisal, Suppressed molecular ionization for a class of diatomics in intense femtosecond laser fields. Phys. Rev. Lett. **85**(11), 2280–2283 (2000)
13. X.M. Tong, Z.X. Zhao, C.D. Lin, Theory of molecular tunneling ionization. Phys. Rev. A **66**(3), 033402 (2002)
14. Bin Zhang, Jianmin Yuan, Zengxiu Zhao, Dynamic core polarization in strong-field ionization of co molecules. Phys. Rev. Lett. **111**(16), 163001 (2013)
15. Domagoj Pavičić, Kevin F. Lee, David M. Rayner, Paul B. Corkum, David M. Villeneuve, Direct measurement of the angular dependence of ionization for n 2, o 2, and co 2 in intense laser fields. Physical review letters **98**(24), 243001 (2007)

16. Lotte Holmegaard, Jonas L. Hansen, Line Kalhøj, Sofie Louise Kragh, Henrik Stapelfeldt, Frank Filsinger, Jochen Küpper, Gerard Meijer, Darko Dimitrovski, Mahmoud Abu-Samha et al., Photoelectron angular distributions from strong-field ionization of oriented molecules. Nat. Phys. **6**(6), 428–432 (2010)

17. K.J. Betsch, D.W. Pinkham, R.R. Jones, Directional emission of multiply charged ions during dissociative ionization in asymmetric two-color laser fields. Phys. Rev. Lett. **105**(22), 223002 (2010)

18. Hui Li, Dipanwita Ray, Sankar De, Irina Znakovskaya, W. Cao, G. Laurent, Z. Wang, Matthias F. Kling, Anh-Thu. Le, C.L. Cocke, Orientation dependence of the ionization of co and no in an intense femtosecond two-color laser field. Phys. Rev. A **84**(4), 043429 (2011)

19. S. Chelkowski, A.D. Bandrauk, Two-step coulomb explosions of diatoms in intense laser fields. J. Phys. B **28**(23), L723 (1995)

20. Haizhen Ren, Ri. Ma, Jianxin Chen, Xia Li, Hong Yang, Qihuang Gong, Field ionization and coulomb explosion of co in an intense femtosecond laser field. Journal of Physics B: Atomic, Molecular and Optical Physics **36**(11), 2179 (2003)

21. Wu. Chengyin, Haizhen Ren, Tingting Liu, Ri. Ma, Hong Yang, Hongbing Jiang, Qihuang Gong, Mass and photoelectron spectrometer for studying field-induced ionization of molecules. Int. J. Mass Spectrometry **216**(3), 249–255 (2002)

22. F. Rosca-Pruna, E. Springate, H.L. Offerhaus, M. Krishnamurthy, N. Farid, C. Nicole, M.J.J. Vrakking, Spatial alignment of diatomic molecules in intense laser fields: I. experimental results. J. Phys. B **34**(23), 4919 (2001)

23. Hongbing Jiang, Wu. Chengyin, Ri. Ma, Juan Huang, Runhai Wang, Hong Yang, Qihuang Gong, Dynamic alignment of co in an intense femtosecond laser field. Chemical physics letters **406**(1–3), 116–120 (2005)

24. Wei Guo, Jingyi Zhu, Bingxing Wang, Yanqiu Wang, Li. Wang, Alignment effects of no in femtosecond laser field. Chem. Phys. Lett. **448**(4–6), 173–177 (2007)

25. K. Zhao, L.N. Elberson, G.M. Menkir, W.T. Hill III., Direct measurement of dynamic alignment in strong fields. Phys. Rev. A **74**(3), 033408 (2006)

26. S. De, Irina Znakovskaya, D. Ray, F. Anis, Nora G. Johnson, I.A. Bocharova, M. Magrakvelidze, B.D. Esry, C.L. Cocke, I.V. Litvinyuk et al., Field-free orientation of co molecules by femtosecond two-color laser fields. Phys. Rev. Lett. **103**(15), 153002 (2009)

27. Chunlei Guo, Observation of selective charge separation following strong-field single ionization. Physical Review A **71**(2), 021405 (2005)

28. Xufei Sun, Min Li, Yun Shao, Ming-Ming. Liu, Xiguo Xie, Yongkai Deng, Wu. Chengyin, Qihuang Gong, Yunquan Liu, Vibrationally resolved electron-nuclear energy sharing in above-threshold multiphoton dissociation of co. Phys. Rev. A **94**(1), 013425 (2016)

29. Wenbin Zhang, Zhichao Li, Lu. Peifen, Xiaochun Gong, Qiying Song, Qinying Ji, Kang Lin, Junyang Ma, Feng He, Heping Zeng et al., Photon energy deposition in strong-field single ionization of multielectron molecules. Phys. Rev. Lett. **117**(10), 103002 (2016)

30. Irina Znakovskaya, P von Den Hoff, Sergey Zherebtsov, Adrian Wirth, Oliver Herrwerth, Marc JJ Vrakking, Regina de Vivie-Riedle, Matthias F Kling Attosecond control of electron dynamics in carbon monoxide. Physical review letters **103**(10), 103002 (2009)

31. J. Wu, L. Ph, H. Schmidt, M. Kunitski, M. Meckel, S. Voss, H. Sann, H. Kim, T. Jahnke, A. Czasch, R. Dörner, Multiorbital tunneling ionization of the co molecule. Phys. Rev. Lett. **108**(18), 183001 (2012)

32. Mingyuan Shi, Shaochuan Huang, Wei Xi, Zuoye Liu, Du. Hongchuan, Baowei Ding, Hu. Bitao, High resolution coulomb explosion spectra and angular distributions of fragment ions of n 2 in a femtosecond laser field. Appl. Phys. B **123**(3), 90 (2017)

33. Guoqiang Shi, Yulin Xiang, Pingquan Wang, Zexuan Wang, Shaohua Sun, Zuoye Liu, Hu. Bitao, Coulomb explosion and angular distributions of the fragment ions of highly charged co in the strong laser field. J. Modern Opt. **68**(1), 10–18 (2021)

34. Chunlei Guo, Ming Li, George N. Gibson, Charge asymmetric dissociation induced by sequential and nonsequential strong field ionization. Phys. Rev. Lett. **82**, 2492–2495 (1999)

35. C. Guo, M. Li, J.P. Nibarger, G.N. Gibson, Single and double ionization of diatomic molecules in strong laser fields. Phys. Rev. A **58**, R4271–R4274 (1998)

36. Jian Zhang, Yan Yang, Zhipeng Li, Haitao Sun, Shian Zhang, Zhenrong Sun, Channel-resolved multiorbital double ionization of molecular cl $_2$ in an intense femtosecond laser field. Phys. Rev. A **98**, 043402 (2018)

37. M. Th Weber, A Staudte Weckenbrock, L. Spielberger, O. Jagutzki, V. Mergel, F. Afaneh, G. Urbasch, M. Vollmer, H. Giessen, R. Dörner, Sequential and nonsequential contributions to double ionization in strong laser fields. J. Phys. B **33**(4), L127–L133 (2000)

38. Robert Locht, The dissociative ionization of carbon monoxide. Chemical Physics **22**(1), 13–27 (1977)

39. G. Ravindra Kumar, Vidhya Krishnamurthi, Deepak Mathur, On the kinetic energy released upon collision-induced dissociation of oriented diatomic ions. Rapid Commun. Mass Spectrometry **7**(8), 734–737 (1993)

40. Akiyoshi Hishikawa, Shilin Liu, Atsushi Iwasaki, Kaoru Yamanouchi, Light-induced multiple electronic-state coupling of o 2+ in intense laser fields. The Journal of chemical physics **114**(22), 9856–9862 (2001)

41. Ch. Ellert, P.B. Corkum, Disentangling molecular alignment and enhanced ionization in intense laser fields. Phys. Rev. A **59**(5), R3170 (1999)

42. Kazutoshi Okada, Suehiro Iwata, Accurate potential energy and transition dipole moment curves for several electronic states of CO. Journal of Chemical Physics **112**(4), 1804–1808 (2000)

43. Wei Xing, Deheng Shi, Jicai Zhang, Jinfeng Sun, Zunlue Zhu, Accurate potential energy curves, spectroscopic parameters, transition dipole moments, and transition probabilities of 21 low-lying states of the CO cation. J. Quantitative Spectrosc. Radiative Transf. **210**, 62–73 (2018)

44. Paul H Krupenie, Stanley Weissman, Potential-energy curves for CO and CO$^+$. The Journal of Chemical Physics **43**(5), 1529–1534 (1965)

45. L.V. Keldysh. Ionization in the field of a strong electromagnetic wave. Sov Phys, **20**, (1965)

46. J. Liu, D.F. Ye, J. Chen, X. Liu, Complex dynamics of correlated electrons in molecular double ionization by an ultrashort intense laser pulse. Phys. Rev. Lett. **99**(1), 013003 (2007)

47. R.W. Nicholls, Franck-condon factors for ionizing transitions of O$_2$, CO, NO and H$_2$ and for the NO$^+$ (a^1-x^1) band system. J. Phys. B **1**(6), 1192 (1968)

48. Xiaokai Li, Yu. Jiaqi, Xu. Huiying, Yu. Xitao, Yizhang Yang, Zhenzhen Wang, Pan Ma, Chuncheng Wang, Fuming Guo, Yujun Yang et al., Multiorbital and excitation effects on dissociative double ionization of CO molecules in strong circularly polarized laser fields. Physical Review A **100**(1), 013415 (2019)

49. Shih-I. Chu, Floquet theory and complex quasivibrational energy formalism for intense field molecular photodissociation. The Journal of Chemical Physics **75**(5), 2215–2221 (1981)

50. A.M. Sayler, P.Q. Wang, K.D. Carnes, B.D. Esry, I. Ben-Itzhak, Determining laser-induced dissociation pathways of multielectron diatomic molecules: application to the dissociation of o 2+ by high-intensity ultrashort pulses. Phys. Rev. A **75**(6), 063420 (2007)

51. X. He, O. Atabek, A. Giusti-Suzor, Laser-induced resonances in molecular dissociation in intense fields. Phys. Rev. A **38**(11), 5586 (1988)